

Cyanide-modified Pt(111): structure, stability and hydrogen adsorption

María Escudero-Escribano^a, Germán J. Soldano^b, Paola Quaino^{b, c}, Martín E. Zoloff Michoff^d, Ezequiel P. M. Leiva^d, Wolfgang Schmickler^b, and Ángel Cuesta^{a,*}

^a*Instituto de Química Física "Rocasolano", CSIC, C. Serrano, 119, E-28006 Madrid, Spain*

^b*Institut für Theoretische Chemie, Universität Ulm, D-89069 Ulm, Germany*

^c*PRELINE, Facultad de Ingeniería Química, Universidad Nacional del Litoral, 3000, Santa Fe, Argentina.*

^d*INFIQC, Departamento de Matemática y Física, Facultad de Ciencias Químicas, Universidad Nacional de Córdoba, Córdoba, Argentina*

*Corresponding autor.

E-mail address: a.cuesta@iqfr.csic.es

Abstract

Cyanide-modified Pt(111) surfaces have been recently used to study atomic-ensemble effects in electrocatalysis. These studies have been based on the assumption that cyanide acts as a third body, blocking some surface sites but leaving the electronic properties of the surrounding ones unaltered, although this is in apparent contradiction with the observation of a positive shift of 0.2 V in the onset of hydrogen adsorption on cyanide-modified Pt(111) electrodes, as compared with clean Pt(111). We have performed theoretical calculations in order to provide support to this assumption and explain the positive shift in the onset of hydrogen adsorption, which is shown to be due to the formation of CNH_{ad} .

Keywords: cyanide-modified Pt(111); DFT; hydrogen adsorption

1. Introduction

The adsorption of cyanide on single-crystal platinum electrodes has been intensively investigated over the last two decades, partly because cyanide and carbon monoxide are isoelectronic [1-10]. Cyanide is irreversibly adsorbed on Pt single-crystal electrodes: the case of Pt(111) is particularly interesting, due to the spontaneous formation, upon immersion of Pt(111) in a cyanide-containing solution, of an ordered $(2\sqrt{3} \times 2\sqrt{3})R30^\circ$ structure [1,4,5] which extends over the whole electrode surface and is composed of hexagonally packed hexagons, each of them containing six cyanide groups adsorbed on top of a hexagon of Pt surface atoms surrounding a free Pt atom. This structure was observed for the first time using low-energy electron diffraction (LEED)

1
2
3
4
5
6
7
8
9
10
11
12
13
14
15
16
17
18
19
20
21
22
23
24
25
26
27
28
29
30
31
32
33
34
35
36
37
38
39
40
41
42
43
44
45
46
47
48
49
50
51
52
53
54
55
56
57
58
59
60
61
62
63
64
65

by Hubbard and co-workers [1], who demonstrated that the $(2\sqrt{3} \times 2\sqrt{3})R30^\circ$ structure formed by adsorbed cyanide on Pt(111) resists electrode emersion and transfer into a UHV chamber, which indicates a very strong adsorption. The atomic, real space structure could later be elucidated by electrochemical STM [4,5]. Although most STM experiments were performed in alkaline solutions [4,5], Itaya and co-workers [5] observed the same structure in acidic solutions.

Cyanide adsorption on Pt(111) has been intensively studied in acidic solutions by Huerta *et al.* [6-10], who demonstrated, by means of cyclic voltammetry, that cyanide-covered Pt(111) could be considered as a chemically-modified electrode [6]. The cyanide adlayer on Pt(111) is remarkably stable, no change being observed upon repetitive cycling between 0.05 and 1.10 V. Cyclic voltammograms (CVs) of cyanide-modified Pt(111) in HClO_4 and in H_2SO_4 solutions are qualitatively very similar, indicating the insensitivity of the chemically-modified surface to the anions present in the supporting electrolyte, *i.e.*, adsorbed cyanide acts as a third-body, which selectively blocks the sites necessary for the adsorption of tetrahedral anions, such as sulphate, on Pt, while leaving unaffected the CN-free Pt atoms onto which OH, CO or NO [10-12] can adsorb.

A very appropriate way to study the role of geometric atomic ensembles in electrocatalysis is to modify the surface in such a way that only one kind of site is removed without modifying the electronic structure of the rest of the surface (the site-knockout strategy [13]). Interestingly, all the sites composed of three contiguous Pt atoms are absent on cyanide-modified Pt(111) and, as a consequence, adsorption at *three-fold hollow* sites [12,14] or reaction steps requiring three contiguous Pt atoms [15,16] are inhibited. These chemically-modified surfaces have been used to demonstrate that the dehydrogenation of methanol [15] and the dehydration of formic acid [16] to adsorbed carbon monoxide require at least three contiguous Pt atoms. Furthermore, modification of Pt(111) with cyanide results in a huge enhancement of the catalytic activity for the ORR in sulfuric and phosphoric acid solutions, because the sites necessary for the adsorption of the tetragonal anions of these acids have been blocked [14]. In all the previous cases, it was assumed that significant simultaneous electronic effects were absent, although we lacked a clear and definitive proof. Cyanide-modified Pt(111) surfaces can also be used to study the role of non-covalent interactions at the electrochemical double layer [17], and cations non-covalently attached to the electrode surface can be used as precursors for surface nanostructuring [18,19].

1 Theoretical studies concerning the spatial and electronic structure, as well as the
2 stability of cyanide-modified Pt(111) surfaces, are needed due to the interest in
3 employing this system to study atomic ensemble effects in electrocatalysis and as a
4 template to fabricate nanostructures on surfaces. Additionally, theoretical calculations
5 are particularly necessary in order to understand the adsorption of hydrogen on cyanide-
6 modified Pt(111) surfaces. The present contribution addresses these points.
7
8
9

10 11 **2. Experimental and computational details**

12 Experimental details have been reported previously [11,12,15-18]. Briefly,
13 cyanide-modified Pt(111) electrodes were prepared by immersion of a clean and well-
14 ordered Pt(111) surface in a 0.1 M KCN (Merck, p.a.) solution for approximately 3 min,
15 after which the electrode was rinsed with ultrapure water and transferred to the
16 electrochemical or spectroelectrochemical cell containing the cyanide-free solutions. A
17 reversible hydrogen electrode (RHE) and a platinum wire were used as reference and
18 counter electrode, respectively. All the potentials in the text are referred to the RHE.
19
20
21
22
23
24
25

26 Calculations were performed either with the DACAPO [20] or the SIESTA [21]
27 DFT codes. In those cases in which the same calculation was performed with both
28 codes, identical results, within the error margins, were obtained. More computational
29 details can be found in the Supporting Information.
30
31
32
33
34

35 **3. Results and discussion**

36 Although the structure of adsorbed cyanide on Pt(111) electrodes has been
37 elucidated by LEED [1] and *in situ* STM [4,5], and although many unique properties of
38 these chemically-modified electrodes have been experimentally proved [6-11], there is a
39 lack of theoretical studies concerning the structure and the configuration adopted by
40 adsorbed cyanide on Pt(111) surfaces. Theoretical calculations are particularly
41 necessary in order to understand (i) the reason why the cyanide adlayer adopts the
42 experimentally observed $(2\sqrt{3} \times 2\sqrt{3})R30^\circ$ structure and (ii) the effect of adsorbed
43 cyanide on the electronic structure of the Pt atoms not directly bonded to CN, and the
44 experimental results regarding the adsorption of hydrogen on cyanide-modified Pt(111).
45
46
47
48
49
50
51
52

53 **3.1. Structure of cyanide adsorbed on Pt(111) surfaces.** In order to study the
54 dependence of the adsorption energy of cyanide on the coverage of CN_{ad} , we have
55 calculated the adsorption energy of adsorbed CN on Pt(111) surfaces for different
56 adsorption sites (*on-top*, *bridge*, *fcc-hollow* and *hcp-hollow*) and various configurations
57
58
59
60
61
62
63
64
65

in the coverage interval between 0.25 and 1 ML. The adsorption energy was calculated taking the substrate and the radical adsorbate as reference (Eq. 1). We have also computed the changes in the work function induced by CN_{ad} on a Pt(111) surface, given by Equation 2, where the sub-index *adsorbate* is referred to CN_{ad} . The calculated work function of the Pt(111) surface obtained using DACAPO is $\Phi_{Pt(111)} = 5.80$ eV.

$$E_{ad} = E_{CN-Pt(111)} - (E_{CN} + E_{Pt(111)}) \quad (1)$$

$$\Delta\Phi = \Phi_{adsorbatePt(111)} - \Phi_{Pt(111)} \quad (2)$$

Figure 1 shows top views of the configurations with CN_{ad} in an *on-top* position for which E_{ad} of cyanide on Pt(111) at $\theta_{CN} = 0.25$ (Figure 1A), $\theta_{CN} = 0.75$ (Figure 1B), and $\theta_{CN} = 1$ (Figure 1C) were calculated. Calculations for the same cyanide coverages with all the CNs in *bridge*, *fcc-hollow* or *hcp-hollow* sites were performed with the same structures by simply shifting the CN groups to the corresponding adsorption site. It must be noted that none of these theoretical structures has been observed experimentally. For the particular case of 0.5 ML, we have calculated the adsorption energy of cyanide for three different configurations: (i) the experimentally observed $(2\sqrt{3} \times 2\sqrt{3})R30^\circ$ structure (Figure 2A), labeled *top(exp)* in Table 1; (ii) a *zig-zag* distribution with all the CN groups adsorbed *on-top* (Figure 2B), that resulted after relaxation of a linear distribution of cyanide in a 2 x 2 unit cell, due to the repulsion between the nitrogen atoms of neighboring CN groups; and (iii) a *mix* structure in which half of the CN groups are adsorbed *on-top* and the other half are adsorbed on *three-fold hollow* sites (Figure 2C), that resulted after relaxation of a 2 x 2 unit cell in which cyanide was adsorbed in the *three-fold hollow* (*fcc* or *hcp*) sites. The calculated adsorption energies for *on-top* and *fcc-hollow* sites corresponding to the configurations illustrated in Figures 1 and 2 are given in Table 1 (note that the results for $\theta_{CN} = 0.75$, corresponding to the configuration in Figure 1B, have not been included in Table 1).

The coverage dependence of the calculated adsorption energy of cyanide adsorbed *on-top* and at *fcc-hollow* sites is shown in Figure 3A. Obviously, the adsorption energy becomes less negative as the coverage increases due to the repulsion between adsorbed CN groups. As can be seen in Table 1 and in Figure 3A, the energy difference between different adsorption sites is too small to explain the experimentally observed preference for adsorption *on-top*, that most likely is due to an additional energy gain by the interaction of the negative charge accumulated on the N atom of the CN moieties with the water dipoles at the interface, which were not included in our calculations.

1
2
3
4
5
6
7
8
9
10
11
12
13
14
15
16
17
18
19
20
21
22
23
24
25
26
27
28
29
30
31
32
33
34
As shown in Figure 3A, the calculated adsorption energy curves for *fcc* and *on-top* sites intercross at $\theta_{\text{CN}} = 0.5$. Figure 3B shows the calculated total electronic density versus the distance from the metal surface (z) for CN_{ad} coverages of 0.25 and 1. At $\theta_{\text{CN}} = 0.25$, the charge density initially decreases fast with the distance from the surface, and then remains more or less constant until it vanishes at distances longer than the nitrogen-surface separation. In contrast, at $\theta_{\text{CN}} = 1$, there is a local maximum at the location of the nitrogen atoms. This electron accumulation is large enough as to produce charge repulsion between the large electronic density of the nitrogen atoms and the electrons of the Pt(111) surface. Since in the case of CN adsorbed *on-top* nitrogen atoms are located farther from the surface, the repulsion is lower, and the calculated adsorption energy is slightly lower for *on-top* sites than for *fcc* sites. This result suggests that the calculated adsorption energy of CN on Pt(111) results from a competition between two types of forces: a chemical force, that tends to locate CN_{ad} on the *fcc* site, and an electrostatic force that tends to push the CN_{ad} further from the surface and favors adsorption *on-top*. The larger dipole moment induced in the case of CN adsorption *on-top* at high coverage, due to the larger charge separation (Figure 3B), will favor the solvation of CN by water molecules, and, as noted above, will contribute to the experimentally observed preference of the CN groups to be adsorbed *on-top*, that, as noted above, cannot be justified based exclusively on our DFT calculations.

35
36
37
38
39
40
41
42
43
44
45
46
47
48
49
50
51
52
53
54
55
56
57
58
59
60
61
62
63
64
65
For all the structures considered in Table 1 the changes in the work function, $\Delta\Phi_{\text{CN}}$, caused by CN adsorption, are large (of the order of a few electron volts) and positive. In an aqueous solution, the large dipole moment of the adsorbed CN groups will induce a net orientation of the water dipoles in the opposite direction, which will partially cancel the surface dipole potential. To get an idea of the magnitude at which the surface dipole may be compensated by the solvent orientation, we can recall the results obtained by one of us [22], who found, for the case of sp metals, a contribution of the solvent to the potential drop across the interface between -0.2 and -0.4 V. These results were confirmed later using semiempirical models for the metal [23] and, in the case of Ag, the solvent contribution was predicted to be of the order of -0.6 V [24], in agreement with experimental work function measurements [25]. More recently, one of us has determined experimentally, for the case of Pt(111) and CO-covered Pt(111) electrodes in 0.1 M HClO_4 , the contribution at the pzc of the interfacial water layer to the potential drop across the interface [26], that was found to be of -1.07 V in the case of Pt(111) and of -0.2 V in the case of Pt(111) covered by a saturated CO adlayer.

1
2
3
4
5
6
7
8
9
10
11
12
13
Nevertheless, in the present case, a net increase of the work function should result, entailing a concomitant shift of the potential of zero charge (pzc) to more positive values. Therefore, the adsorption of cations will set in at more positive electrode potentials than at the bare Pt(111) electrodes. The larger changes in the work function upon adsorption of cyanide when *on-top* sites are occupied at different CN coverages, including the $(2\sqrt{3} \times 2\sqrt{3})R30^\circ$ structure observed experimentally, as compared with CN adsorbed on *fcc-hollow* sites, are also due to the larger dipole moment of CN_{ad} in the former case.

14
15
16
17
18
19
20
21
22
23
24
25
26
27
28
29
30
31
32
33
34
35
36
37
38
39
40
41
42
43
44
45
46
47
48
49
50
51
52
53
54
55
56
57
58
59
60
61
62
63
64
65
As can be seen in Figure 2A, a pseudo-hexagonal arrangement of the adsorbed cyanide groups results after relaxation of the experimentally observed $(2\sqrt{3} \times 2\sqrt{3})R30^\circ$ structure of cyanide-modified Pt(111), due to the tendency of the nitrogen atoms to be as far from each other as possible, causing the CN groups not to be perpendicular to the metal surface. The adsorption energy calculated for the relaxed $(2\sqrt{3} \times 2\sqrt{3})R30^\circ$ structure is -3.17 eV (Table 1), and is very close in energy to the other two alternative configurations with the same θ_{CN} (Table 1): the *zig-zag* distribution, shown in Figure 2B ($E_{ad} = -3.10$ eV), and the *mix* structure (Figure 2C, $E_{ad} = -3.23$ eV). The slightly higher stability of the latter structure is mainly due to the location of the CN groups at different heights above the metal surface (Figure 2C), which lowers the repulsion between the N atoms of two neighboring CN groups. These results indicate that, from a thermodynamical point of view, equilibrium between the three structures described above should be expected. However, as indicated above, only the $(2\sqrt{3} \times 2\sqrt{3})$ structure has been experimentally observed. A cation located at the center of each hexagonal cyanide ring of the $(2\sqrt{3} \times 2\sqrt{3})$ structure, as suggested by Itaya and co-workers based on their STM images [5] in solutions containing K^+ or Na^+ , could explain the tendency of CN_{ad} to form an ordered array of hexagons, instead of distributing themselves over the surface with a homogeneous CN-CN separation. However, according to our DFT calculations of the adsorption energy of alkaline metal cations (approximated as neutral metals) on different adsorption sites (Table 2), the centre of the CN hexagonal rings (one adsorbed cation per unit cell, Figure 4A) is the most favorable site in the case of K, but adsorption at the $(CN)_3$ sites (honeycomb structure, Figure 4B) is the most favorable in the case of Na. In both cases, adsorption at the $(CN)_4$ sites (Figure 4C, kagome structure) is the least favorable. (A kagome lattice is an arrangement of lines composed of interlaced triangles, such that each point where two lines cross has four neighboring similar crossing points. See, e.g, Fig. 4C and Fig. 5.) We would like to note here that, in

1 the first-principles calculations method that we have used, no particular assumption is
2 made on the status of charge of the cations. In this way, they acquire the charge
3 determined by the energy minimization of the energy functional with respect to the
4 electric density. In this respect, it is interesting to point out that the cations do take, as
5 chemical intuition dictates, a large positive charge, as can be noted in the sixth column
6 of Table 2.
7
8
9

10
11 In any case, we have strong grounds to affirm that cations, which are always
12 present during the experimental formation of the cyanide adlayer, may play an
13 important role in determining the structure of cyanide-modified Pt(111) electrodes.
14 Experimental evidence of the presence of cations attached to the cyanide-modified
15 Pt(111) has been reported even under UHV conditions by *ex situ* LEED experiments
16 [1]. Our recent quantitative study of non-covalent interactions between alkali-metal
17 cations and the CN groups of cyanide-modified Pt(111) electrodes has shown that a
18 good match between the size of the cation and that of the cavity in which it has to be
19 accommodated is critical in determining the cation's adsorption energy [17]. A
20 comparison of the *zig-zag* and the *mix* structures with the $(2\sqrt{3} \times 2\sqrt{3})$ structure suggests
21 that the size of the different cavities available for the adsorption of cations plays a
22 crucial role in determining the optimized configuration. The *mix top-fcc* arrangement,
23 which is the most stable according to the theoretical calculations, does not seem a stable
24 candidate for the adsorption of cations due to the large size of the cavity formed by a
25 trigonal arrangement of Pt atoms. As for the *zig-zag* structure, although the cavity in
26 this case is quite similar to that of the experimentally observed structure, in the presence
27 of counter-ions the CN groups probably tend to rearrange, rendering a distribution less
28 stable than the $(2\sqrt{3} \times 2\sqrt{3})$ structure.
29
30
31
32
33
34
35
36
37
38
39
40
41
42

43
44 3.2. Hydrogen adsorption on cyanide-modified Pt(111) surfaces. The double layer-
45 corrected voltammetric charge in the hydrogen adsorption region of a cyanide-modified
46 Pt(111) electrode amounts to *ca.* $80 \mu\text{C cm}^{-2}$, which is the charge expected for the
47 adsorption of atomic hydrogen on two thirds of the Pt atoms left free upon modification
48 of the Pt(111) electrode with cyanide, in very good agreement with Huerta *et al.* [7],
49 who suggested that adsorbed cyanide blocks only some of the sites available for
50 hydrogen adsorption. Interestingly, on cyanide-modified Pt(111) the onset of hydrogen
51 adsorption is shifted positively by *ca.* 0.20 V with respect to unmodified Pt(111)
52 electrodes (Figure S1). This implies that ΔG_0 of H_{upd} ($\theta_{\text{H}} = 0$) is *ca.* 19 kJ mol^{-1} more
53
54
55
56
57
58
59
60
61
62
63
64
65

1 negative on cyanide-modified Pt(111) [12], and might suggest a modification of the
2 electronic structure of the free Pt atoms in the cyanide-modified Pt(111) surface. As we
3 will show below, this is not the case. Actually, the onset of hydrogen evolution does not
4 seem to be affected by the presence of CN_{ad} on cyanide-modified Pt(111) electrodes
5 (Figure S1), onto which *on-top* sites, thought to be the active ones in the evolution of H_2
6 on Pt(111) electrodes, are perfectly available. If these sites remain electronically
7 unaltered, hydrogen evolution would be expected to coincide on both Pt(111) and
8 cyanide-modified Pt(111) electrodes.
9

10 The shift in the onset of hydrogen adsorption can be explained by the formation
11 in the H_{upd} region of adsorbed hydrogen isocyanide, CNH_{ad} , instead of H_{ad} directly
12 bonded to the Pt atoms. This idea had been already proposed by Schardt *et al.* [27], who
13 suggested that the CNH_{ad} adlayer behaves as a polyprotic acid. The formation of
14 $(\text{CN}_{\text{ad}})_x\text{-H}$ (with x decreasing with decreasing potential within the H adsorption region)
15 would explain all the previous experimental facts. As can be observed in Figure 5, the
16 charge density at the broad peak at 0.48 V in the H_{upd} region is *ca.* $20 \mu\text{C cm}^{-2}$ ($\theta_{\text{CNH}} =$
17 $1/12 \text{ ML}$), which might correspond to a $(\text{CN}_{\text{ad}})_6\text{-H}$ stoichiometry. The minimum of
18 current density at *ca.* 0.40 V corresponds to a charge density of about $32 \mu\text{C cm}^{-2}$ (θ_{CNH}
19 $= 1/8 \text{ ML}$), coinciding with the charge expected for the formation of $(\text{CN}_{\text{ad}})_4\text{-H}$. Finally,
20 at 0.37 V and *ca.* 0.20 V, the charge densities are $40 \mu\text{C cm}^{-2}$ ($\theta_{\text{CNH}} = 1/6 \text{ ML}$) and
21 $64 \mu\text{C cm}^{-2}$ ($\theta_{\text{CNH}} = 0.25 \text{ ML}$), respectively. The former may correspond to a $(\text{CN}_{\text{ad}})_3\text{-H}$
22 stoichiometry (honeycomb structure), and the latter to a $(\text{CN}_{\text{ad}})_2\text{-H}$ stoichiometry
23 (kagome structure).
24

25 Itaya and co-workers [5] attributed the STM images of a cyanide-modified
26 Pt(111) electrode obtained at 0.30 V vs. RHE (well within the H_{upd} region) in perchloric
27 acid solutions to a $(\sqrt{7} \times \sqrt{7})R19^\circ$ structure, but this is in contradiction with the absence
28 in the cyclic voltammogram of any feature indicating a phase transition, as would be
29 expected for a change from a long-range ordered $(2\sqrt{3} \times 2\sqrt{3})R30^\circ$ structure to a long-
30 range ordered $(\sqrt{7} \times \sqrt{7})R19^\circ$ structure. As shown in Figure 5, the structure found by
31 Itaya and co-workers can also be interpreted as a kagome structure, in excellent
32 agreement with our analysis above, based on the charge density measured in the
33 corresponding CV.
34

35 The IR spectra of cyanide adsorbed on Pt(111) electrodes have been intensively
36 studied both in acidic [6,7] and in alkaline solutions [3,4,28,29]. The spectra show a
37 single vibrational band corresponding to the stretching vibration of a CN group
38
39

1 adsorbed *on-top* of a platinum atom through its carbon atom [3,4,6,7]. A plot of the CN_L
2 stretching frequency of cyanide-modified Pt(111) vs. the electrode potential (Figure S2)
3 shows two clearly different slopes: at $E \leq 0.5$ V the CN_L stretching frequency increases
4 with potential with a slope of $82 \text{ cm}^{-1} \text{ V}^{-1}$, this being significantly smaller than that of
5 ca. $100 \text{ cm}^{-1} \text{ V}^{-1}$ reported by Huerta *et al.* [6,7], while for $E \geq 0.60$ V the slope is 25 cm^{-1}
6 V^{-1} , in good agreement with the literature [6,7]. Some authors attributed this change in
7 the Stark tuning rate to a change from N-bound CN at $E \leq 0.50$ V to C-bound CN at $E >$
8 0.50 V [6,7,30], and this assignment was supported by theoretical calculations of Pt-CN⁻
9 and Pt-NC⁻ vibrational systems [31,32]. In contrast, Paulissen and Korzeniewski [2]
10 suggested that the changes in the Stark tuning rate correspond to the conversion from
11 Pt-CN to Pt-CNH species. Naturally, due to bond order conservation, the adsorption of
12 hydrogen on the nitrogen atoms of adsorbed cyanide should weaken the carbon-nitrogen
13 bond, and hence decrease the corresponding C-N stretching vibrational frequency. A
14 comparison of the plot of the CN_L stretching frequency of cyanide-modified Pt(111) vs.
15 the electrode potential (Figure S2) with the CV of the cyanide-modified Pt(111)
16 electrode (Figure S1) strongly suggests that the high slope at $E \leq 0.50$ V must be due to
17 the presence of hydrogen protonating the nitrogen atoms of the adsorbed cyanide.
18 Therefore, our hypothesis is that over the whole frequency range between 2085 and
19 2123 cm^{-1} the band of the cyanide-modified Pt(111) corresponds to C-bound CN
20 adsorbed on-top on Pt(111) and that the change in the Stark tuning rate of the CN
21 stretching frequency at ca. 0.50 V, coinciding with the onset of hydrogen adsorption in
22 the cyclic voltammogram, can be explained by the formation of (CN_{ad})_x-H.
23
24
25
26
27
28
29
30
31
32
33
34
35
36
37
38
39

40 We have analyzed the projected density of states (PDOS) of the topmost Pt
41 atoms, in order to identify the electronic factors that control the adsorption of CN on
42 Pt(111) surfaces, and in order to prove our assumption that the electronic structure of
43 the surface Pt atoms that are not directly bonded to CN remains essentially unaltered.
44 Figure 6A shows the DOS projected on the carbon atom of a CN_{ad} and on the Pt atom of
45 the cyanide-modified Pt(111) surface bonded to it. As can be observed there is a
46 resonance of Pt/CN states at around -16 eV, where the 2sp states of carbon and the 6sp
47 states of platinum clearly overlap. A contribution of the d states of Pt can also be
48 detected at around -7.5 eV.
49
50
51
52
53
54
55
56

57 The DOS projected on the *d*-band of the surface Pt atoms of a cyanide-modified
58 Pt(111) electrode with the $(2\sqrt{3} \times 2\sqrt{3})\text{R}30^\circ$ structure (Figure 6B), shows that the PDOS
59
60
61
62
63
64
65

of the Pt atoms directly bonded to the CN_{ad} is shifted to lower energies as compared to clean Pt(111), this being consistent with a strong bonding. On the other hand, the DOS projected on the d -band of the free Pt atoms remains nearly identical to the PDOS of the Pt atoms of the clean (111) surface, supporting the notion that CN_{ad} acts as an inert site blocker. Hence, the positive shift in the onset potential for hydrogen adsorption cannot be explained by an electronic disturbance of the free Pt atoms of the cyanide-modified Pt(111) surface.

As a first approximation, we calculated the adsorption energies at low coverage (1/9 ML) of the CN radical (Eq. 1) and of H (Eq. 3) onto a clean Pt(111) surface and of H onto a Pt(111) surface with a low coverage of adsorbed CN ($\theta = 1/9$ both for H and for CN), both on a free Pt atom (Eq. 4) and protonating the N atom of a CN group (Eq. 5). Figure 7 illustrates the low-coverage structures for which these calculations were performed, Table 3 summarizes the relevant information concerning the adsorption of H onto a clean Pt(111) surface, and Table 4 that for the adsorption of CN and for the adsorption of H onto a Pt(111) surface with 1/9 ML of CN. The adsorption energies for H are calculated with respect to a H_2 molecule (Eqs. 3-5).

$$E_{\text{ad}}^{\text{H-Pt}} = E_{\text{H-Pt(111)}} - \left(\frac{E_{\text{H}_2}}{2} + E_{\text{Pt(111)}} \right) \quad (3)$$

$$E_{\text{ad}}^{\text{H-Pt}} = E_{\text{H-Pt(111)-CN}} - \left(\frac{E_{\text{H}_2}}{2} + E_{\text{NC-Pt(111)}} \right) \quad (4)$$

$$E_{\text{ad}}^{\text{H-NC-Pt}} = E_{\text{H-NC-Pt(111)}} - \left(\frac{E_{\text{H}_2}}{2} + E_{\text{NC-Pt(111)}} \right) \quad (5)$$

The adsorption energy of CNH on Pt(111) is calculated according to Eq. 6:

$$E_{\text{ad}} = E_{\text{CNH-Pt(111)}} - (E_{\text{CNH}} + E_{\text{Pt(111)}}) \quad (6)$$

The CN adsorption energies in Table 4 are consistent with those shown in Table 1, although the latter were calculated with DACAPO and the former with SIESTA. Interestingly, the energy of adsorption of hydrogen on the free Pt atoms of a Pt(111) surface with a low coverage of CN (Table 4, Figure 7C) is similar to that on the different sites of a clean Pt(111) surface (Table 3, Figure 7A), and nearly half the energy corresponding to the protonation of the nitrogen atom of Pt(111)-CN to form Pt(111)-CNH (Table 4, Figure 7B). This is in agreement with the result of the PDOS in Figure 6 and with our hypothesis that the shift of 0.2 V in the onset of hydrogen

1
2
3
4
5
6
7
8
9
10
11
12
13
14
15
16
17
18
19
20
21
22
23
24
25
26
27
28
29
30
31
32
33
34
35
36
37
38
39
40
41
42
43
44
45
46
47
48
49
50
51
52
53
54
55
56
57
58
59
60
61
62
63
64
65

adsorption on cyanide-modified Pt(111), as compared to clean Pt(111), is due to the formation of CNH_{ad} .

We have also studied the adsorption energy of CNH on Pt(111), given by Equation 6, at different coverages, and have compared it with the adsorption energy of CN on Pt(111), given by Equation 1. We have also computed the changes in the work function induced by CNH_{ad} on a Pt(111) surface using Equation 2, where the sub-index *adsorbate* is now referred to CNH_{ad} . The results of these calculations are shown in Table 5.

The value for the adsorption energy of 0.25 ML of CNH on Pt(111) in Table 5 is in very good agreement with the value obtained for 0.19 ML of CNH in Table 4, although the former was obtained with DACAPO and the latter with SIESTA. Table 5 shows that the adsorption of CNH_{ad} inverts the dipole moment of the surface with respect to CN_{ad} (Table 1). As happens with CN_{ad} , large differences in the work function changes are found for CNH_{ad} in the different configurations studied, in contrast with the small change in the adsorption energy found for the same coverages of CNH_{ad} (Table 5). The positive values calculated for $\Delta\Phi_{(\text{CNH})}$ using DACAPO (Table 5) are in agreement with the positive total charge on the CNH_{ad} species inferred from the Mulliken analysis, obtained using SIESTA, in Table 4.

The adsorption energy of hydrogen on Pt(111) covered by CN with $\theta_{\text{CN}} = 0.25$ (Figures 8A, 8B, 9A and 9B) and $\theta_{\text{CN}} = 0.5$ (Figures 8C, 8D, 9C and 9D), both on the nitrogen atom of adsorbed cyanide (Figure 8) and on the Pt atoms of the Pt(111) surface (Figure 9), was also calculated according to Equations 5 and 7. The results are summarized in Table 6. Although the *zig-zag* arrangement is one of the most stable configurations for 0.5 ML of CN on Pt(111), as can be observed in Table 1, for CNH_{ad} it becomes unfavourable, because the CNH groups rearrange in a linear configuration in order to favour the formation of hydrogen bonds between neighbouring adsorbates (Figures 8C and D), that add additional stability to the adlayer and cannot be formed in the *zig-zag* configuration. It must be noted that the values of $E_{\text{ads}}^{\text{H-Pt}}$ shown in Table 6 and calculated with Eq. 7 correspond to the adsorption of H on the free Pt atoms of Pt(111)- CNH_{ad} , when hydrogen is already adsorbed on the nitrogen atom of the CN groups. We have checked that the difference of these results with respect to $E_{\text{ad}}^{\text{H-Pt}}$ on Pt(111)- CN_{ad} , i.e., when H is not bonded to the nitrogen atom of the CN groups, is negligible (lower than 0.1 eV). This is confirmed by the similitude between the energy

of adsorption of H on a free Pt atom in Table 4 and in Table 6, although in the former case the calculation was performed with SIESTA and in the latter with DACAPO, and despite the differences in θ_{CN} and θ_{H} .

$$E_{\text{ad}}^{\text{H-Pt}} = E_{\text{HNC-HPt(111)}} - \left(\frac{E_{\text{H}_2}}{2} + E_{\text{HNC-Pt(111)}} \right) \quad (7)$$

Although none of the structures for which $E_{\text{ad}}^{\text{H-Pt}}$ was calculated in Table 6 corresponds to the experimentally observed $(2\sqrt{3} \times 2\sqrt{3})$ structure, the results corroborate that the adsorption of hydrogen on the free Pt atoms of the different structures of cyanide-modified Pt(111) is very close in energy to the adsorption on unmodified Pt(111), as already deduced from the results of the calculation of the *d*-band PDOS (Figure 6) and from the results in Table 4. These results show that hydrogen adsorbed on the nitrogen atom of CN_{ad} is between ca. 0.5 and ca. 1 eV more stable than hydrogen adsorbed on the free Pt atoms of the cyanide-modified Pt(111) surface, and strongly support the hypothesis that the hydrogen adsorption region on cyanide-modified Pt(111) is due to the formation of $(\text{CN}_{\text{ad}})_x\text{-H}$.

In addition to the calculations above, that involve surface structures not observed experimentally, the adsorption of H onto the experimentally observed Pt-CN $(2\sqrt{3} \times 2\sqrt{3})R30^\circ$ surface was also investigated, both in the presence and in the absence of a competing species such as K. The adsorption of H onto the free Pt atoms of a Pt-CN $(2\sqrt{3} \times 2\sqrt{3})R30^\circ$ surface was studied at a low coverage ($\theta = 1/12$) of H, because the onset of hydrogen adsorption, for which a positive shift of 0.20 V is observed in the case of cyanide-modified Pt(111), corresponds to the limit of zero coverage. The different possible adsorption modes that were assessed include H on *top* of the free Pt atoms considering the three different possible sites: (i) **Pt-(CN)₃**, a free Pt with 3 first neighbors with a CN_{ad} (Figure 10A); (ii) **Pt-(CN)₄**, a free Pt with 4 first neighbors with a CN_{ad} (Figure 10B); and (iii) **Pt-(CN)₆**, a free Pt with 6 first neighbors with a CN_{ad} (Figure 10C). We also tried to adsorb H on hollow sites. On the Pt-CN $(2\sqrt{3} \times 2\sqrt{3})R30^\circ$ surface there are no hollow sites surrounded by three free Pt atoms, but it contains hollow sites composed of either 2 free Pt and 1 Pt-CN_{ad} or 1 free Pt and 2 Pt-CN_{ad} . When an H atom was placed on one of these hollow sites, we observed two different behaviors: the H atom left the surface, and it either protonated a N atom or a C atom. In the latter case, the resulting HCN molecule desorbed from the surface.

1 We also studied H adsorption at the N atoms of the CN_{ad} of a Pt-CN ($2\sqrt{3} \times$
2 $2\sqrt{3}$) $R30^\circ$ surface, varying the H coverage between 1/12 (**Pt-CN-Hx1**, Figure 10D) and
3 1/4 (with respect to the surface Pt atoms). For $\theta = 1/4$, two different stable structures
4 were found, which we have called **Pt-CN-Hx3 geom-1** (Figure 10E) and **Pt-CN-Hx3**
5 **geom-2** (Figure 10F). Finally, H adsorption on top of the free Pt atoms was also
6 examined in the presence of non-covalently attached K forming a *honeycomb* adlayer
7 [17], and in the presence of a non-covalently attached K adlayer with the *centre of the*
8 *ring* structure. The results of these calculations are summarized in Table 7.

9 Interestingly, protonation of the N atoms of the adsorbed CNs of the ($2\sqrt{3} \times$
10 $2\sqrt{3}$) $R30^\circ$ structure is energetically very favorable, with an adsorption energy more than
11 1 eV larger than H bonded to the CN-free Pt atoms, which is barely affected by the
12 presence of K and whose adsorption energy (Table 7) is roughly the same as on clean
13 Pt(111) (Table 3). Formation of $(\text{CN}_{\text{ad}})_x\text{-H}$ explains, hence, the experimentally observed
14 0.2 V positive shift of the onset of hydrogen adsorption. Our calculations also confirm
15 that the effect of the alkaline cations on the CV of a cyanide modified Pt(111) electrode
16 can be explained by a competition for the same adsorption sites, as we have suggested
17 recently [17].

18 Finally, as illustrated in Figure 11 and as suggested by the high value of the
19 hydrogen adsorption energy of the Pt-CN-Hx1 structure (Figure 10D and Table 2), the
20 formation of $(\text{CN}_{\text{ad}})_x\text{-H}$ is probably further stabilized by the formation of hydrogen-
21 bonds between nitrogen atoms of neighboring cyanide groups in the hexagonal ring, as
22 happens with the linear configuration (Figures 8C and D).

23 Our theoretical calculations show that hydrogen adsorption *on top* of the free Pt
24 atoms of the CN_{ad} -covered Pt(111) surface is also thermodynamically stable for all the
25 configurations analyzed (Tables and 4, 6 and 7). This supports the idea that, in the
26 potential region between 0.6 V and 0.1 V, hydrogen adsorbs on the nitrogen atoms of
27 the cyanide groups, but, at sufficiently negative potentials, and once all the available
28 CN_{ad} sites have been occupied, hydrogen can also adsorb directly on the metal, and
29 probably acts as the intermediate species in H_2 evolution.

30 **4. Conclusions**

31 DFT calculations cannot explain by themselves the preference for the
32 experimentally observed structure adopted by cyanide on Pt(111) electrodes, suggesting
33 that adsorption of cyanide forming a ($2\sqrt{3} \times 2\sqrt{3}$) $R30^\circ$ structure is driven by the

1
2
3
4
5
6
7
8
9
10
11
12
13
14
15
16
17
18
19
20
21
22
23
24
25
26
27
28
29
30
31
32
33
34
35
36
37
38
39
40
41
42
43
44
45
46
47
48
49
50
51
52
53
54
55
56
57
58
59
60
61
62
63
64
65

presence of cations, other structures isoenergetic with it presenting cavities with sizes or geometries inappropriate for hosting the cations.

DFT calculations of the DOS projected onto those Pt atoms that are not directly bonded to CN show that the electronic structure of these atoms remains essentially unaltered, which demonstrates that CN_{ad} acts as an inert site blocker. For this reason, cyanide-modified Pt(111) electrodes are unique for studying atomic ensemble effects in electrocatalysis using the site-knockout strategy.

According to DFT calculations, protonation of the nitrogen atoms of CN_{ad} on Pt(111) is clearly favored over adsorption on a Pt atom. The positive shift in the onset of hydrogen adsorption in the CV of cyanide-modified Pt(111) electrodes can, hence, be qualitatively explained by the formation of $(\text{CN}_{\text{ad}})_x\text{-H}$, instead of H bonded to the Pt atoms that remain free in the $(2\sqrt{3} \times 2\sqrt{3})R30^\circ$ cyanide-modified Pt(111) structure. An analysis of the FTIR spectra shows that the Stark tuning rate of the CN stretching frequency of cyanide-modified Pt(111) changes at a potential coinciding with the onset of hydrogen adsorption in the corresponding CV, which can also be explained by the formation of $(\text{CN}_{\text{ad}})_x\text{-H}$.

Acknowledgements

A.C. acknowledges the support of the DGI (Spanish Ministry of Science and Innovation) through Project CTQ2009–07017. W.S acknowledges financial support by the Deutsche Forschungsgemeinschaft under Schm 344/40-1, Schm 344/34-1.2 and FOR 1376. W.S. and P.Q. thank DFG-CONICET International Cooperation and CONICET for continued support. E.P.M.L. and M.Z.-M. wish to acknowledge CONICET PIP: 112-200801-000983, Secyt UNC, Program BID (PICT 2006 N 946), and PME: 2006-01581 for financial support. P.Q. acknowledges PICT 0737-2008. A generous grant of computing time from the Baden-Wuerttemberg grid is gratefully acknowledged. M.E.-E. acknowledges an FPI fellowship from the Spanish Ministry of Science and Innovation and an accommodation grant at the Residencia de Estudiantes from the Madrid City Council.

References

- [1] J.L. Stickney, S.D. Rosasco, G.N. Salaita, A.T. Hubbard, *Langmuir* 1 (1985) 66.
- [2] V.B. Paulissen, C. Korzeniewski, *J. Phys. Chem.* 96 (1992) 4563.
- [3] C.S. Kim, C. Korzeniewski, *J. Phys. Chem.* 97 (1993) 9784.
- [4] C. Stuhlmann, *Surf. Sci.* 335 (1995) 221.
- [5] Y.-G. Kim, S.-L. Yau, K. Itaya, *J. Am. Chem. Soc.* 118 (1996) 393.

- [6] F. Huerta, E. Morallón, C. Quijada, J.L. Vázquez, A. Aldaz, *Electrochim. Acta* 44 (1998) 943.
- [7] F.J. Huerta, E. Morallón, J. Vazquez, A. Aldaz, *Surf. Sci.* 396 (1998) 400.
- [8] F. Huerta, E. Morallón, C. Quijada, J.L. Vázquez, L.E.A. Berlouis, J. *Electroanal. Chem.* 463 (1999) 109.
- [9] F. Huerta, E. Morallón, J.L. Vázquez, *Surf. Sci.* 431 (1999) L577.
- [10] F. Huerta, E. Morallón, J.L. Vázquez, *Electrochem. Commun.* 4 (2002) 251.
- [11] I. Morales-Moreno, A. Cuesta, C. Gutiérrez, *J. Electroanal. Chem.* 560 (2003) 135.
- [12] A. Cuesta, M. Escudero, *Phys. Chem. Chem. Phys.* 10 (2008) 3628.
- [13] A. Cuesta, *ChemPhysChem* 12 (2011) 2375.
- [14] D. Strmcnik, M. Escudero-Escribano, K. Kodama, V.R. Stamenkovic, A. Cuesta, N.M. Markovic, *Nature Chem.* 2 (2010) 880.
- [15] A. Cuesta, *J. Am. Chem. Soc.* 128 (2006) 13332.
- [16] A. Cuesta, M. Escudero, B. Lanova, H. Baltruschat, *Langmuir* 25 (2009) 6500.
- [17] M. Escudero-Escribano, M.E. Zoloff Michoff, E.P.M. Leiva, N.M. Marković, C. Gutiérrez, Á. Cuesta, *ChemPhysChem* 12 (2011) 2230.
- [18] M. Escudero, J.F. Marco, A. Cuesta, *J. Phys. Chem. C* 113 (2009) 12340.
- [19] M. Escudero-Escribano, PhD Thesis, Universidad Autónoma de Madrid, 2011, <http://hdl.handle.net/10261/42378>.
- [20] B. Hammer, L.B. Hansen, J.K. Nørskov, *Phys. Rev. B* 59 (1999) 7413.
- [21] J.M. Soler, E. Artacho, J.D. Gale, A. García, J. Junquera, P. Ordejón, D. Sánchez-Portal, *J. Phys. Condens. Matter.* 14 (2002) 2745.
- [22] W. Schmickler, *Chem. Phys. Lett.* 99 (1983) 135.
- [23] M.I. Rojas, E.P.M. Leiva, *J. Electroanal. Chem.* 303 (1991) 55.
- [24] M.I. Rojas, E.P.M. Leiva, *Surf. Sci.* 227 (1990) L121.
- [25] K. Bange, T.E. Madey, J.K. Sass, E.M. Stuve, *Surf. Sci.* 183 (1987) 334.
- [26] A. Cuesta, *Surf. Sci.* 572 (2004) 11.
- [27] B.C. Schardt, J.L. Stickney, D.A. Stern, D.G. Frank, J.Y. Katekaru, S.D. Rosasco, G.N. Salaita, M.P. Soriaga, A.T. Hubbard, *Inorg. Chem.* 24 (1985) 1419.
- [28] W. Daum, K.A. Friedrich, C. Klünker, D. Knabben, U. Stimming, H. Ibach, *Appl. Phys. A* 59 (1994) 553.
- [29] K.A. Friedrich, W. Daum, C. Klünker, D. Knabben, U. Stimming, H. Ibach, *Surf. Sci.* 335 (1995) 315.
- [30] F. Huerta, F. Montilla, E. Morallón, J.L. Vázquez, *Surf. Sci.* 600 (2006) 1221.
- [31] A. Tadjeddine, A. Peremans, A. Le Rille, W.Q. Zheng, M. Tadjeddine, J.-P. Flament, *J. Chem. Soc. Faraday Trans.* 92 (1996) 3823.
- [32] M. Tadjeddine, J.P. Flament, *Chem. Phys.* 240 (1999) 39.

Figure 1. Top views of the different structures with $\theta_{\text{CN}} = 0.25$ (A), $\theta_{\text{CN}} = 0.75$ (B), and $\theta_{\text{CN}} = 1$ (C) for which the adsorption energy of cyanide adsorbed *on-top* on Pt(111) has been calculated.

Figure 2. Top and side views of the structures with $\theta_{\text{CN}} = 0.5$ for which the adsorption energy of cyanide on Pt(111) has been calculated: (A) Experimentally observed $(2\sqrt{3} \times 2\sqrt{3})R30^\circ$ structure; (B) (2×2) *zig-zag* structure; (C) (2×2) *mix* structure.

Figure 3. A) Adsorption energy of CN_{ad} on Pt(111) at different coverages from 0.25 to 1 ML, with all the CNs occupying either *fcc-hollow* sites (black stars) or *on-top* sites (red circles) and adopting the structures shown in Figure 1. B) Total electronic density (ρ_e) as a function of the distance (z) from the metal surface for cyanide-modified Pt(111). The Pt surface corresponds to $z = 0$. The total charge density for adlayers with

all the CNs at fcc-hollow and at on-top sites are compared for $\theta_{\text{CN}} = 0.25$ (top) and $\theta_{\text{CN}} = 1$ (bottom).

Figure 4. Top view of the three possible cavity sites at which cations can adsorb on the experimentally observed $(2\sqrt{3} \times 2\sqrt{3})R30^\circ$ structure of cyanide-modified Pt(111) surfaces: A) $(\text{CN}_{\text{ad}})_6$, B) $(\text{CN}_{\text{ad}})_3$ and C) $(\text{CN}_{\text{ad}})_4$ cavities.

Figure 5. Left: Cyclic voltammogram at 50 mV s^{-1} of CN-modified Pt(111) in 0.1 M HClO_4 . Right: $5 \times 5 \text{ nm}^2$ STM image obtained at 0.3 V , reprinted and adapted with permission from reference [9], copyright 1996 American Chemical Society. The image can be interpreted as a kagome structure corresponding to a $(\text{CN}_{\text{ad}})_2\text{-H}$ stoichiometry.

Figure 6. A) DOS projected on the C atom of a CN_{ads} group of the $(2\sqrt{3} \times 2\sqrt{3})R30^\circ$ structure and on the Pt atom bonded to it. The sp states of carbon are contrasted with, from top to bottom, the s, p, and d valence states of the metal. B) DOS of the d band projected on the surface atoms of a clean Pt(111) and of a cyanide-modified Pt(111) surface with the experimentally observed $(2\sqrt{3} \times 2\sqrt{3})R30^\circ$ structure. For the cyanide-modified Pt(111) surface, Pt free atoms (not bonded to adsorbed cyanide) are distinguished from the Pt atoms directly bonded to CN (Pt occupied).

Figure 7: A) H adsorbed on a *hollow fcc* site on Pt(111). B) CN adsorbed *on top* protonated on the N atom. C) CN adsorbed *on top* and H adsorbed at a site intermediate between *bridge* and *hcp-hollow*, resulting from the relaxation of a structure in which H was originally adsorbed at one of the *fcc-hollow* sites adjacent to the adsorbed CN group.

Figure 8. Top view of the different configurations for which the adsorption energy of hydrogen on the nitrogen atoms of CN_{ad} of CN-Pt(111) surfaces has been calculated.

Figure 9. Top view of the different configurations for which the adsorption energy of hydrogen on the free Pt atoms of CNH-Pt(111) surfaces has been calculated.

Figure 10: Hydrogen adsorption on the experimentally observed $(2\sqrt{3} \times 2\sqrt{3})R30^\circ$ structure of cyanide-modified Pt(111) surfaces. A) Pt- $(\text{CN})_3\text{-H}$, H_{upd} on top of free Pt with 3 first neighbors Pt- CN_{ad} . B) Pt- $(\text{CN})_4\text{-H}$, H_{upd} on top of free Pt with 4 first neighbors Pt- CN_{ad} . C) Pt- $(\text{CN})_6\text{-H}$, H_{upd} on top of free Pt with 6 first neighbors Pt- CN_{ad} . D) Pt-CN-Hx1, H protonating the N atom of the CN adlayer with $\theta = 1/12$. E) Pt-CN-Hx3 geom-1, H protonating the N atom of the CN adlayer with $\theta = 1/4$. The red hexagon indicates the CN ring, that has deformed as one CN_{ad} has shifted from an *ontop* to a *bridge* position. F) Pt-CN_{Hx3} geom-2, H protonating the N atom of the CN adlayer with $\theta = 1/4$. G) Pt-CN-K(*centre*)-H(CN_4), H_{upd} on a free Pt at a Pt- CN_4 site in the presence of a K adlayer with the cation located at centre of the CN ring. H) Pt-CN-K(*honeycomb*)-H(CN_6), H_{upd} on a free Pt at a Pt- CN_6 site in the presence of a K honeycomb adlayer and I) Pt-CN-K(*honeycomb*)-H(CN_4), H_{upd} on a free Pt at a Pt- CN_4 site in the presence of a K honeycomb adlayer.

Figure 11. Top view of a fully protonated $(2\sqrt{3} \times 2\sqrt{3})R30^\circ$ cyanide-modified Pt(111) surfaces.

Table 1. Adsorption energy (E_{ads}) and work function difference ($\Delta\Phi$) in eV for different configurations and coverages of the CN adlayer on Pt(111) surfaces.

$\theta_{\text{adsorbate}}$	Adsorption site	$E_{\text{ads(CN)}} / \text{eV}$	$\Delta\Phi_{\text{(CN)}} / \text{eV}$
0.25	<i>top</i>	-3.39	2.75
0.25	<i>fcc</i>	-3.47	1.67
0.50	<i>top (exp.)</i>	-3.17	3.56
0.50	<i>top (zig-zag)</i>	-3.10	3.48
0.50	<i>top (linear)</i>	-3.02	3.48
0.50	<i>fcc (linear)</i>	-3.04	2.09
0.50	<i>top-fcc (mix)</i>	-3.23	3.24
1	<i>top</i>	-2.51	3.82
1	<i>fcc</i>	-2.23	3.33

Table 2. Adsorption energies, relevant structural parameters, and Mulliken charge analysis for the three possible structures for Na⁺ and K⁺ adsorbed on the CN-modified Pt(111) surface.

Structure	$E_{\text{ad}} / \text{eV}$ [a]	$d(\text{M}^+ \text{-Pt}) / \text{nm}$ [b]	$d(\text{N-M}^+) / \text{nm}$ [c]	$d(\text{N-Pt}) / \text{nm}$ [d]	δ_{M^+} / e [e]	δ_{CN} / e [e]
M = Na						
Kagome	- 5.31	0.369	0.259	0.314	+ 0.88	- 0.42
Honeycomb	- 5.59	0.423	0.243	0.314	+ 0.88	- 0.32
(CN _{ads}) ₆ -Na ⁺	-5.35	0.391	0.322	0.319	+0.90	-0.22
M = K						
Kagome	- 5.42	0.386	0.265	0.314	+ 0.85	- 0.40
Honeycomb	- 5.62	0.444	0.261	0.314	+ 0.90	- 0.32
(CN _{ads}) ₆ -K ⁺	-5.82	0.445	0.275	0.319	+0.90	-0.24

[a] Adsorption energy referred to the optimized ($2\sqrt{3} \times 2\sqrt{3}$)R30° CN adlayer and a M atom in the vacuum.

[b] Distance between the cation and the Pt surface in the optimized structure.

[c] Averaged distance between M⁺ and the N atom of the CN groups surrounding the adsorption site.

[d] Average distance from the N atoms of the adsorbed CN groups to the Pt surface.

[e] Mulliken charge of the species in the optimized structure.

Table 3. Adsorption energy (E_{ads}), distance of the adsorbed H to the surface and Mulliken charge on the adsorbed H atom ($\theta_{\text{H}} = 1/9$) for the different adsorption sites on Pt(111).

Adsorption site	E_{ads}/eV	$d \text{ H-Pt(111) / nm}$	Mulliken charge on H
<i>top</i>	-0.54	0.159	-0.22
<i>bridge</i>	-0.58	0.105	-0.28
<i>hollow-fcc</i>	-0.63	0.088	-0.27
<i>hollow-hcp</i>	-0.59	0.089	-0.27

Table 4. Adsorption energy (E_{ads}), structural parameters and Mulliken charges for the CN radical adsorbed *on-top* on Pt(111) at low coverage, and for the H atom adsorbed on the nitrogen atom of the CN (Pt(111)-CNH) and at a Pt site intermediate between *bridge* and *hcp-hollow* (NC-Pt(111)-H) in the presence of a low coverage of CN_{ad} .

Structure	E_{ads}/eV		Atomic distances / nm			Mulliken charges	
Pt(111)-CN ^{a)}	CN: -3.59		Pt-C: 0.194	C-N: 0.120	CN: -0.20		
Pt(111)-CNH ^{b)}	CNH: -1.86	H: -0.92	Pt-C: 0.189	C-N: 0.119	N-H: 0.101	CN: +0.38	H: -0.14
NC-Pt(111)-H ^{c)}	CN: -3.54	H: -0.55	Pt-C: 0.194	C-N: 0.120	Pt-H:0.100	CN: -0.23	H: -0.20

^{a)} CN adsorbed *on-top* of a Pt(111) atom, $\theta = 1/9$. ^{b)} CNH adsorbed *on-top* of a Pt(111) atom, $\theta = 1/9$ (Figure 7B); the value given for CNH in column two corresponds to the E_{ads} of a CNH molecule on Pt(111) calculated with Eq. 6, while the value given for H corresponds to E_{ads} of a H atom on the N atom of an adsorbed CN moiety calculated with Eq. 5. ^{c)} CN and H adsorbed *on-top* and on a site intermediate between *bridge* and *hcp-hollow*, respectively (Figure 7C); the value given for CN in column two corresponds to the E_{ads} of a CN radical on Pt(111) calculated with Eq. 1, while the value given for H corresponds to E_{ads} of a H atom on a CN-free Pt atom ($\theta_{\text{H}} = 1/9$) of a Pt(111) surface covered by 1/9 ML of CN, calculated with Eq. 4.

Table 5. Adsorption energy (E_{ads}) and work function difference ($\Delta\Phi$) in eV for different configurations and coverages of a CNH adlayer on Pt(111) surfaces.

$\theta_{\text{adsorbate}}$	Adsorption site	$E_{\text{ads(CNH)}} / \text{eV}$	$\Delta\Phi_{\text{(CNH)}} / \text{eV}$
0.25	<i>top</i>	-1.86	-2.66
0.25	<i>fcc</i>	-2.11	-0.88
0.50	<i>top (zig-zag)</i>	-1.43	-3.37
0.50	<i>top (linear)</i>	-1.60	-2.23
0.50	<i>fcc (linear)</i>	-1.81	-0.86
0.50	<i>top-fcc (mix)</i>	-1.87	-2.38
1	<i>top</i>	-1.04	-2.69
1	<i>fcc</i>	-0.96	-1.63

Table 6. Adsorption energy and work function difference in eV for H adsorbed on N (H-N) or on the Pt surface (H-Pt) forming different configurations and coverages on Pt(111) surfaces.

$\theta_{\text{adsorbate}}$	Adsorption site	$E_{\text{ads}}^{\text{H-N}} / \text{eV}$	$E_{\text{ads}}^{\text{H-Pt}} / \text{eV}$	$\Delta\Phi_{\text{(H-N)}} / \text{eV}$	$\Delta\Phi_{\text{(H-Pt)}} / \text{eV}$
0.25	<i>top</i>	-1.10	-0.31	-2.66	-2.84
0.25	<i>fcc</i>	-1.26	-0.33	-0.68	-1.16
0.50	<i>top (linear)</i>	-0.95	-0.40	-2.23	-2.33
0.50	<i>fcc (linear)</i>	-1.31	-0.28	-0.86	-0.90
0.50	<i>top-fcc (mix)</i>	-1.26	-	-	-

Table 7. Hydrogen and potassium adsorption energy on the $(2\sqrt{3} \times 2\sqrt{3})R30^\circ$ cyanide-modified Pt(111) surface (E_{ads}), structural parameters and Mulliken charges for the structures illustrated in Figure 10.

Structure	E_{ads}/eV	Atomic distances / nm		Mulliken charges
H_{upd}				
Pt-(CN) ₆ -H	H_{upd} : -0.42	H-Pt: 0.159		H: -0.11; CN: -0.20
Pt-(CN) ₄ -H	H_{upd} : -0.33	H-Pt: 0.159		H: -0.02; CN: +0.38
Pt-(CN) ₃ -H	H_{upd} : -0.36	H-Pt: 0.160		H: -0.03; CN: -0.23
Pt-CN-K(<i>honeycomb</i>)- H(CN ₆)	H_{upd} : -0.38 K: -5.60	H-Pt: 0.159	K-Pt: 0.445	H: -0.13; CN: -0.14; K: +0.90
Pt-CN-K(<i>honeycomb</i>)- H(CN ₄)	H_{upd} : -0.30 K: -5.60	H-Pt: 0.159	K-Pt: 0.446	H: -0.12; CN: -0.33; K: +0.90
Pt-CN-K(<i>centre</i>)-H(CN ₄)	H_{upd} : -0.49 K: -5.98	H-Pt: 0.159	K-Pt: 0.393	H: -0.06; CN: -0.22; K: 0.86
H protonating CN				
Pt-CN-Hx1	H: -2.28	H-N: 0.113		H: -0.15; CN(H): +0.25; CN---(H): -0.03; CN: -0.18 ^{a)}
Pt-CN-Hx3 geom-1	H: -1.94	H-N: 0.108		H: -0.11; CN(H): +0.10; CN: -0.10
Pt-CN-Hx3 geom-1	H: -1.73	H-N: 0.105		H: -0.09; CN(H): +0.10 CN: -0.23

^{a)} CN(H) stands for protonated CN_{ad}, CN---(H) stands for the CN that makes a H-bond with the adsorbed H atoms, and CN are the remaining CN_{ad}, that are not involved in the bonding with the H atom.

Figure 1
[Click here to download high resolution image](#)

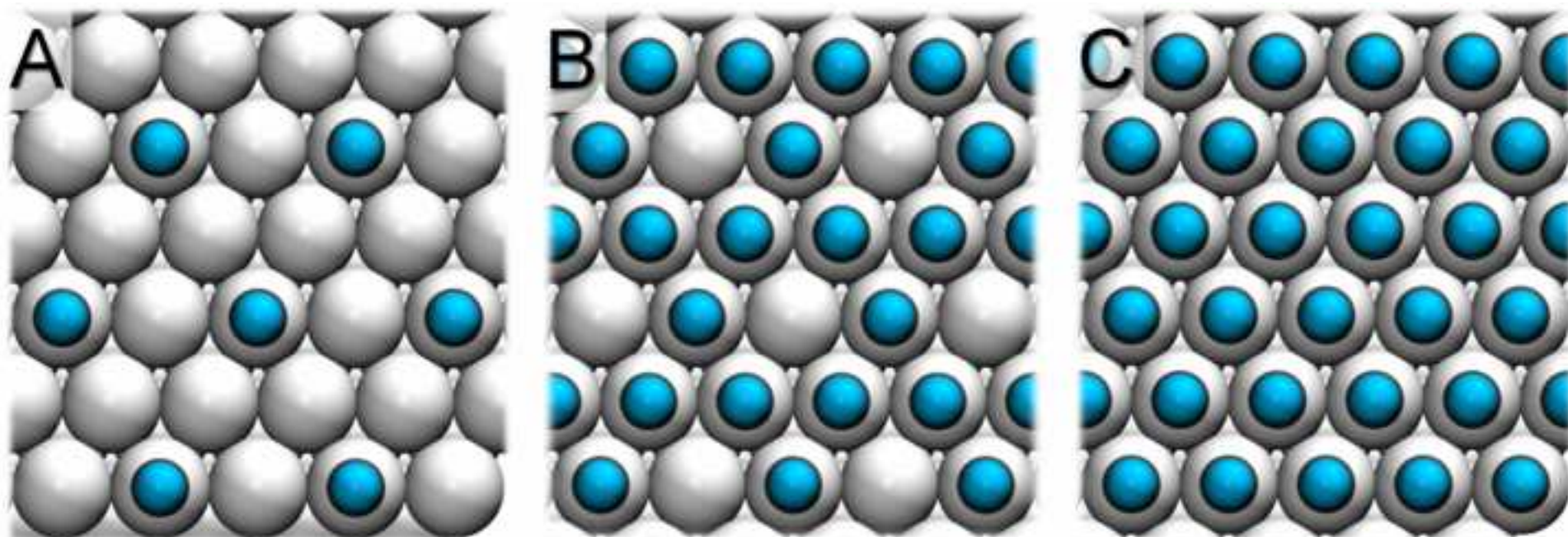


Figure 2
[Click here to download high resolution image](#)

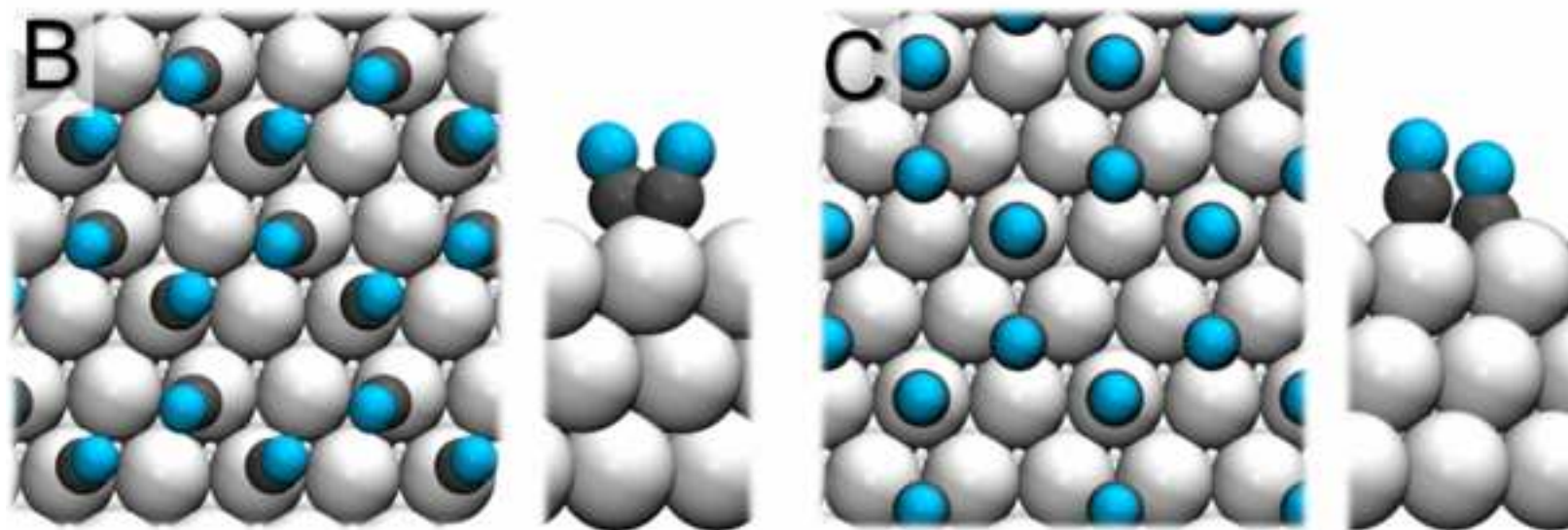
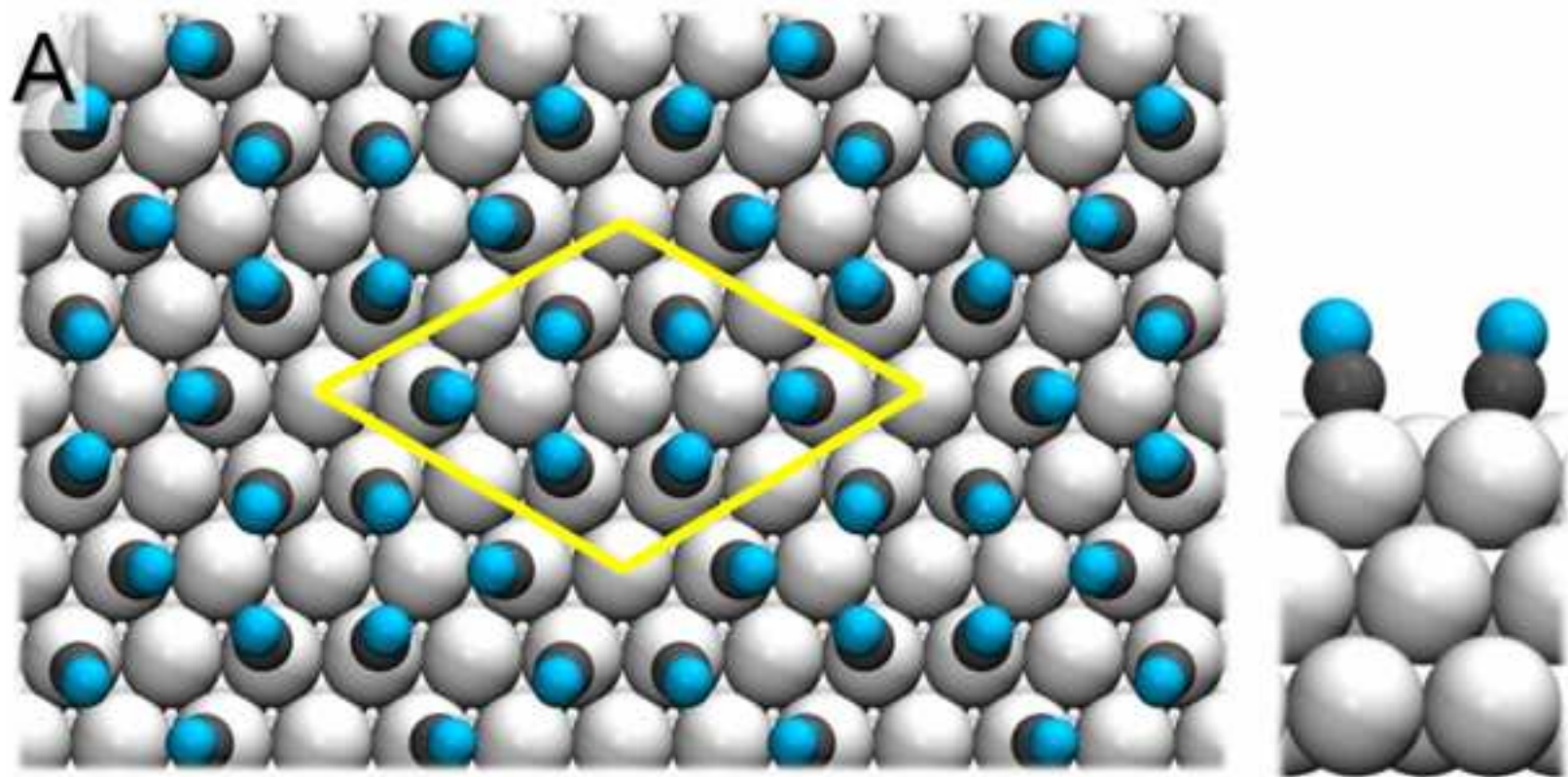


Figure 3
[Click here to download high resolution image](#)

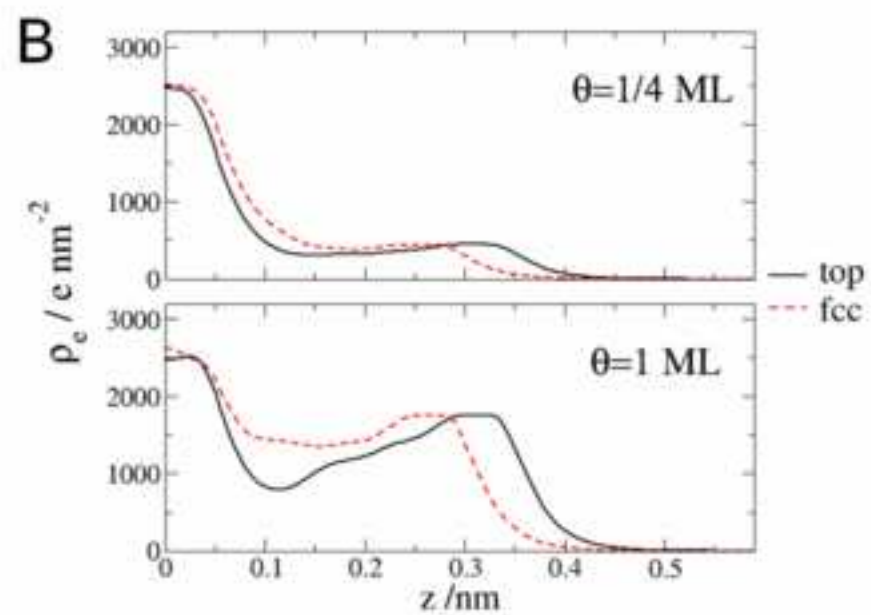
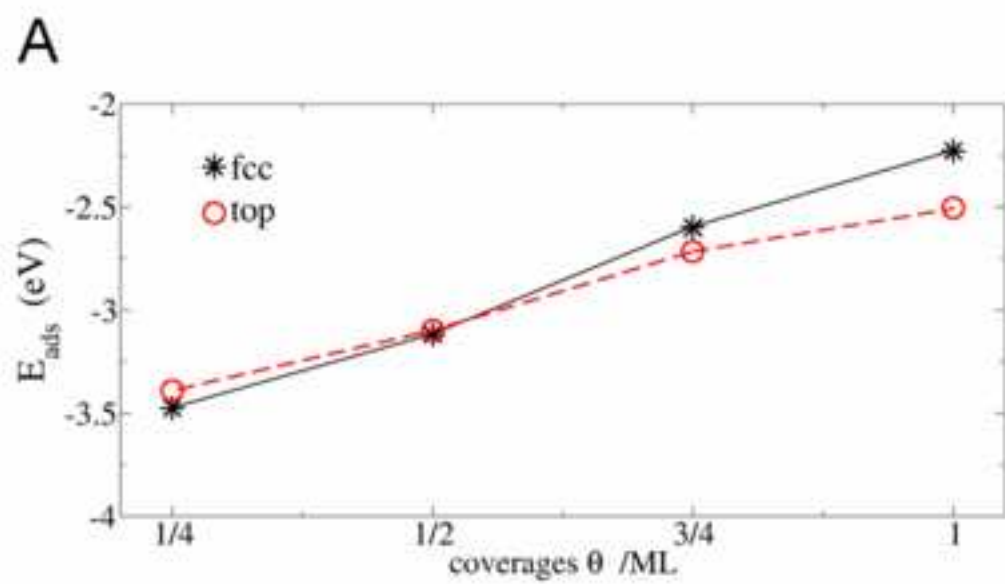


Figure 4
[Click here to download high resolution image](#)

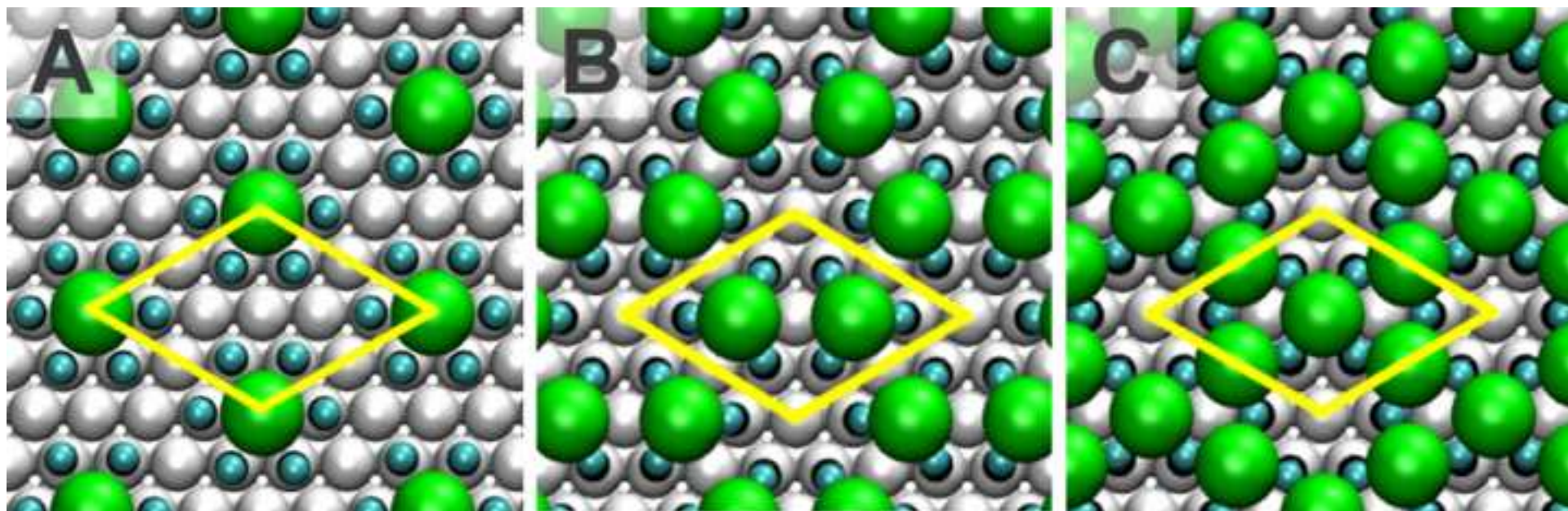


Figure 5
[Click here to download high resolution image](#)

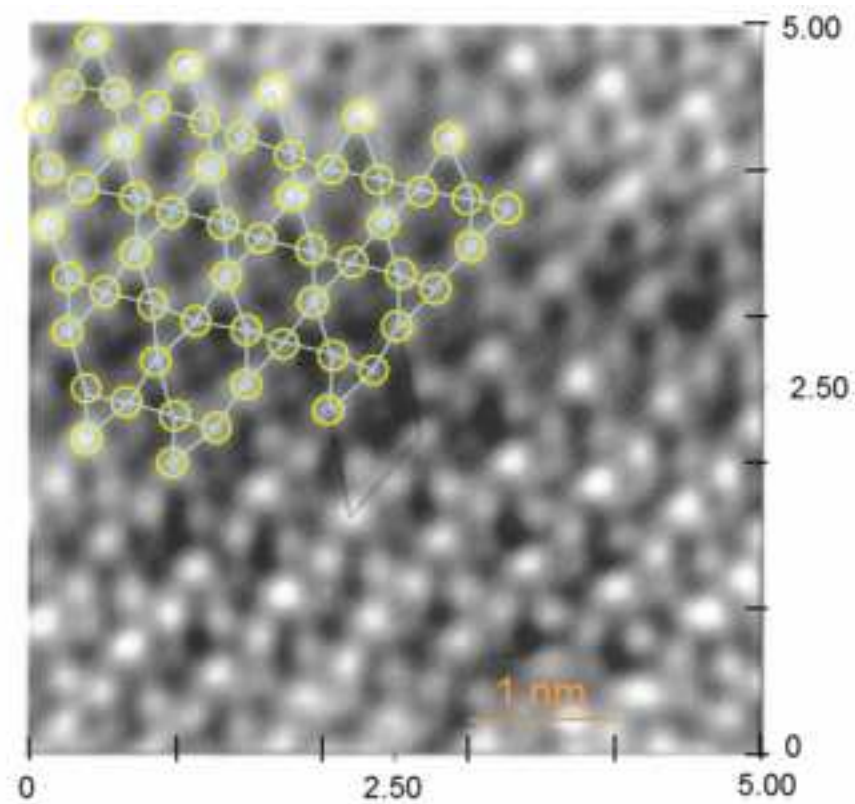
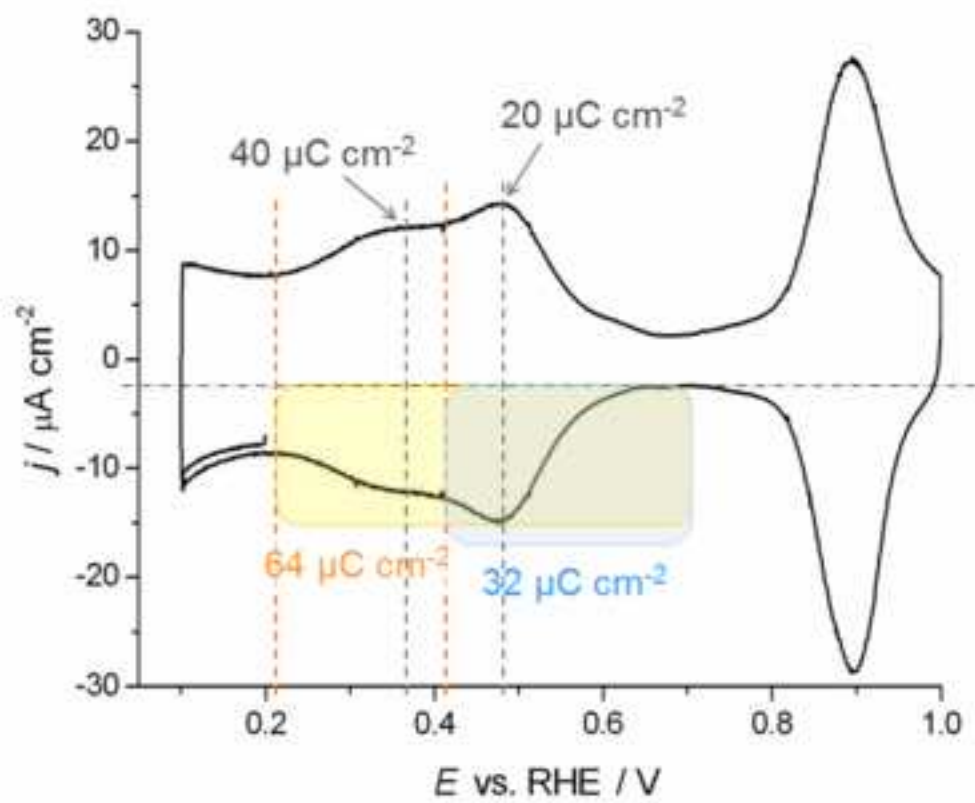


Figure 6
[Click here to download high resolution image](#)

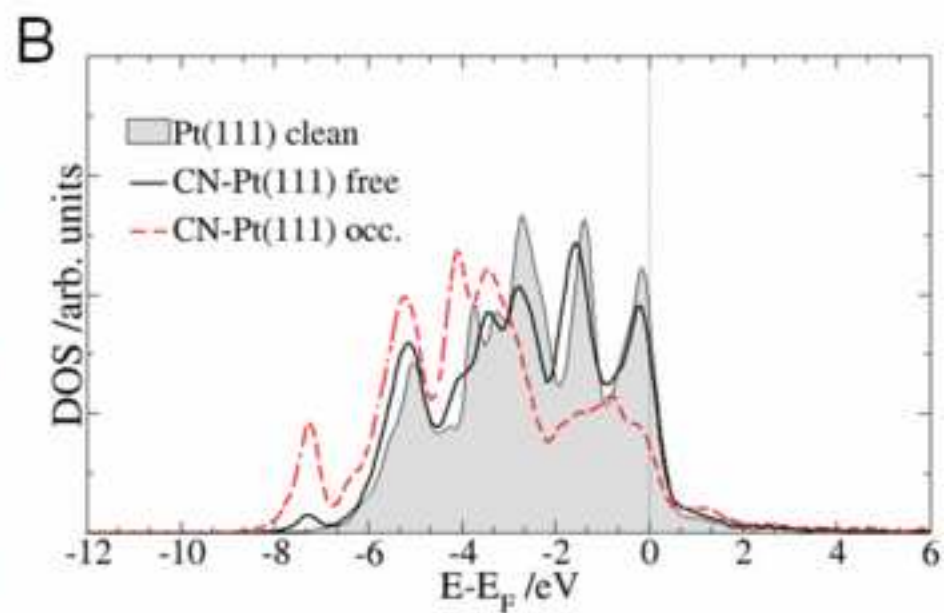
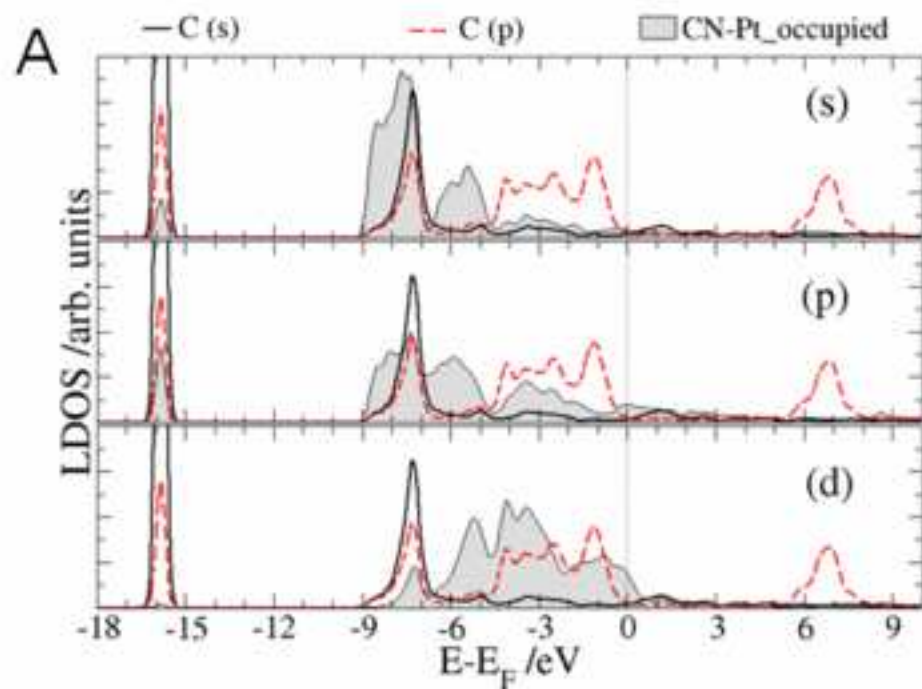


Figure 7
[Click here to download high resolution image](#)

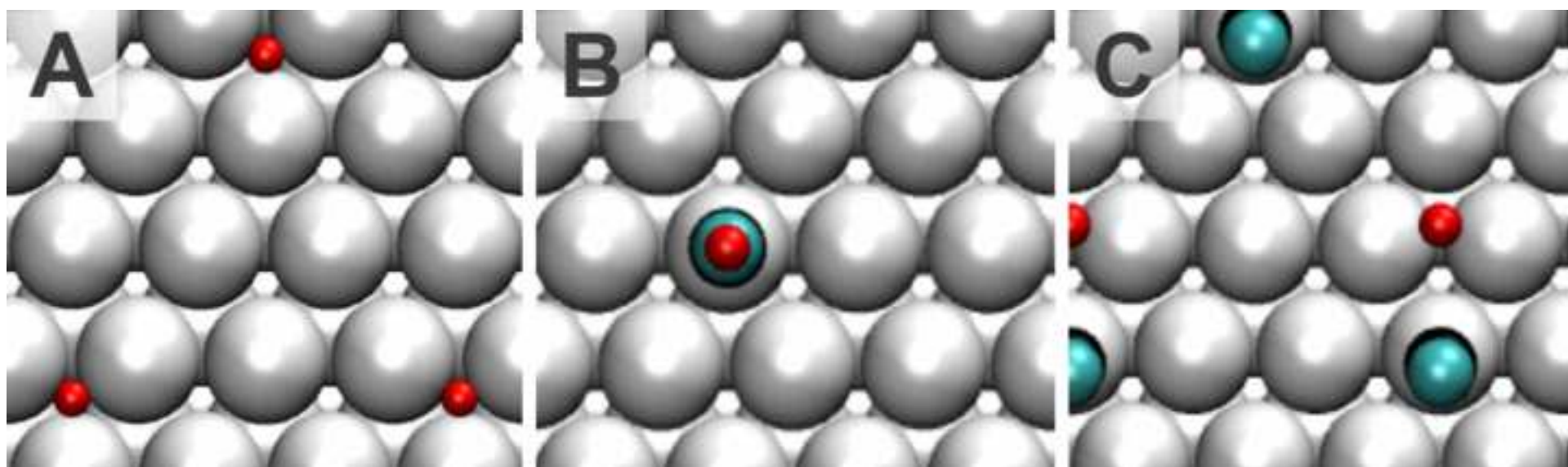


Figure 8
[Click here to download high resolution image](#)

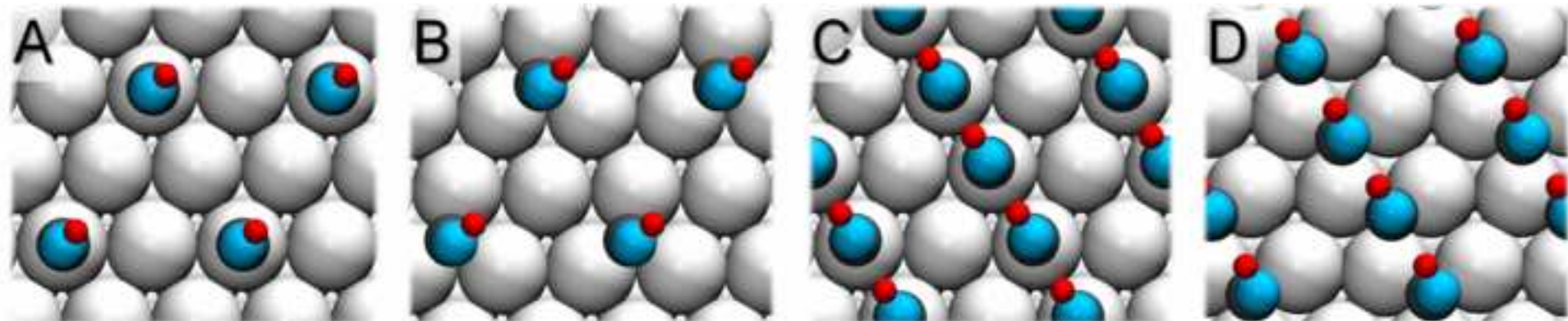


Figure 9
[Click here to download high resolution image](#)

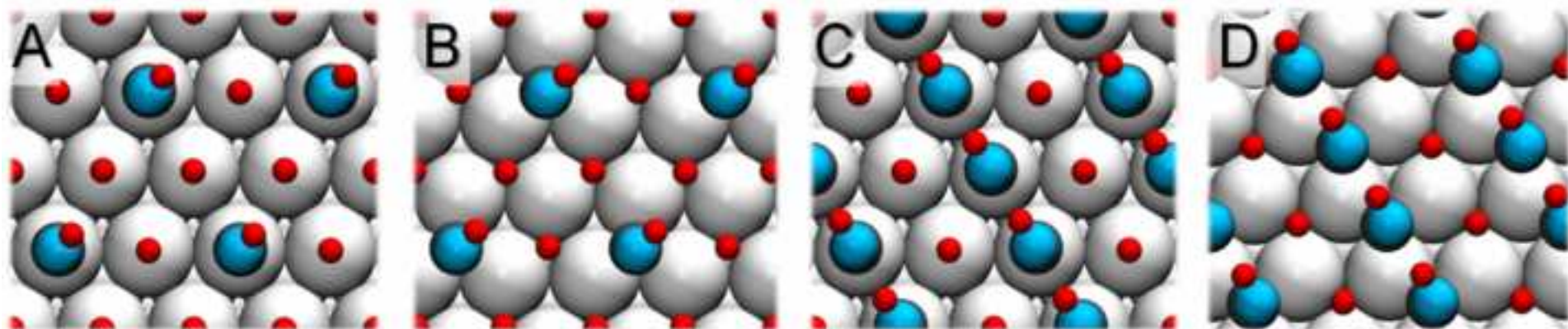


Figure 10
[Click here to download high resolution image](#)

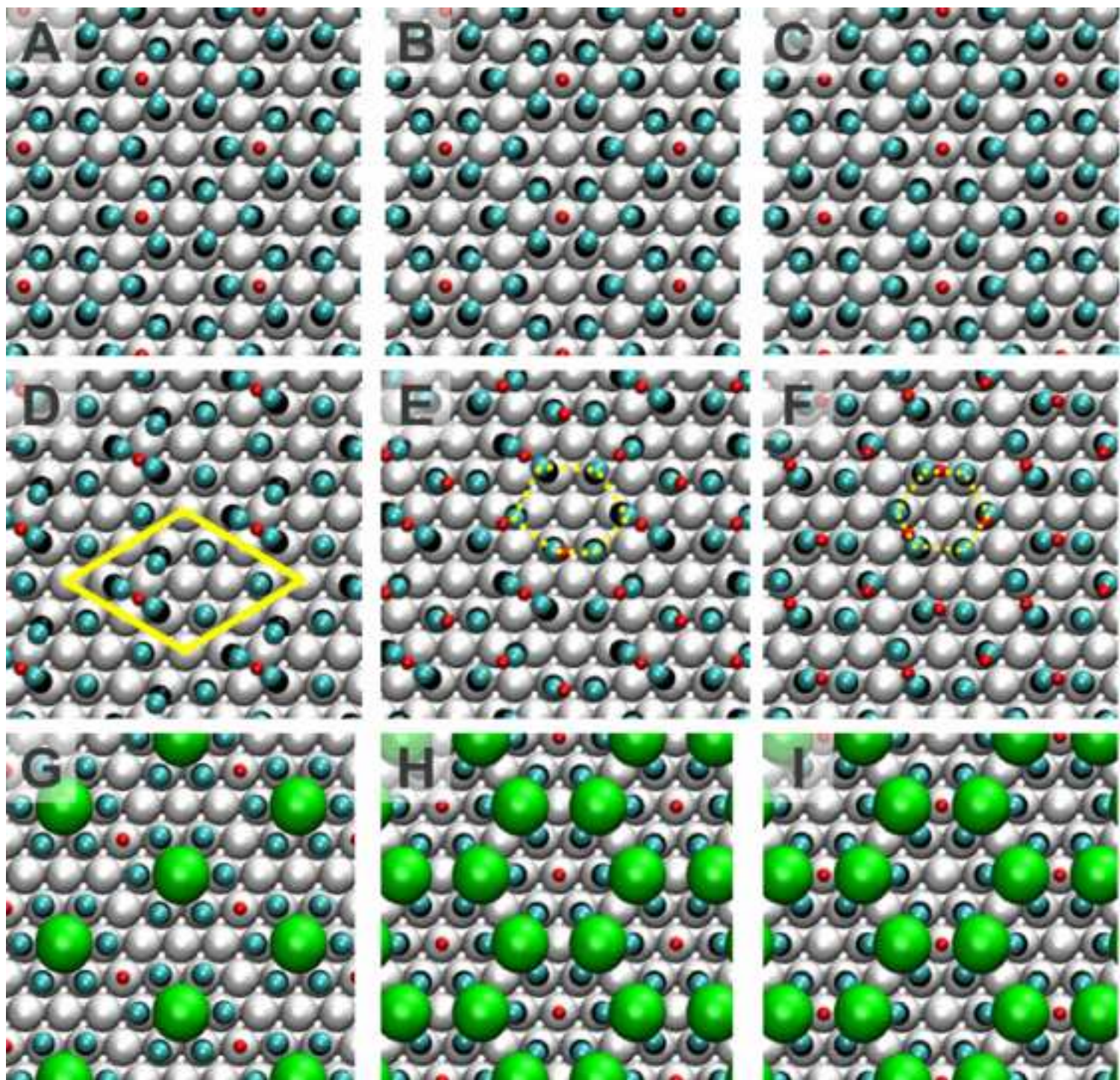
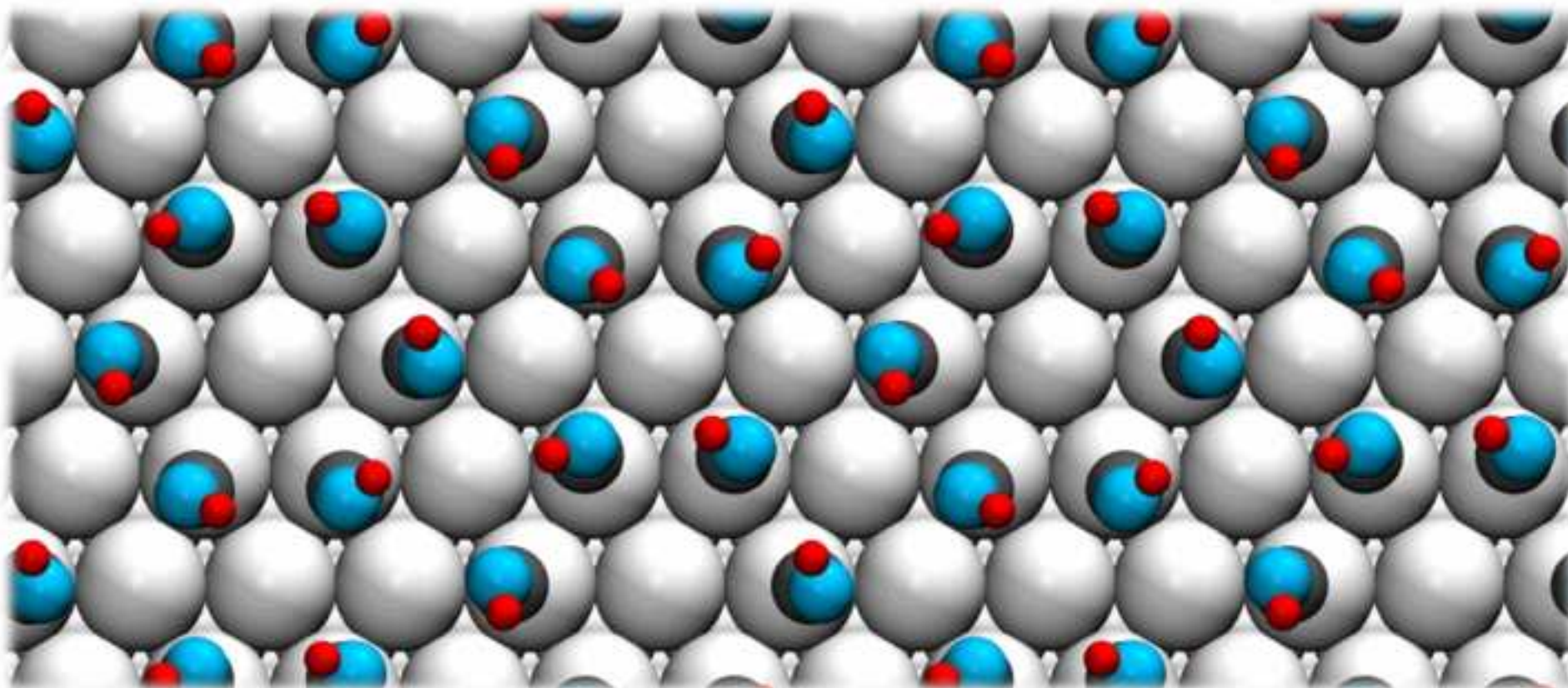


Figure 11
[Click here to download high resolution image](#)



Supporting Information for publication

[Click here to download Supplementary Materials: SI, Escudero-Escribano et al, definitive.doc](#)

Copyright permission for publisher, corresponding to Figure 5B

[Click here to download Supplementary Materials: copyright permission.pdf](#)